ACS APPLIED MATERIALS & INTERFACES

Research Article

www.acsami.org

Substrate-Independent Method for Growing and Modulating the Density of Polymer Brushes from Surfaces by ATRP

Bryan R. Coad,*[,†,‡,§,⊥] Yi Lu,[†] Veronica Glattauer,[†,‡] and Laurence Meagher[†,‡]

[†]CSIRO Materials Science and Engineering, Clayton, Victoria, Australia

[‡]Cooperative Research Centre for Polymers, Notting Hill, Victoria, Australia

[§]Ian Wark Research Institute and [⊥]Mawson Institute, University of South Australia, Mawson Lakes, South Australia

Supporting Information

ABSTRACT: We describe a method for grafting PEG-based polymer chains of variable surface density using a substrate independent approach, allowing grafting from virtually any material substrate. The approach relies upon initial coupling of a macroinitiator to plasma polymer treated surfaces. The macroinitiator is a novel random terpolymer containing ATRP initiator residues, strongly negatively charged groups, and carboxylic acid moieties that facilitate covalent surface anchoring. Surface-initiated ATRP (SI-ATRP) using polyethylene glycol methyl ether methacrylate (PEGMA) at different concentrations led to grafted surfaces of controlled thickness in either the "brush" or "mushroom" morphology, which was controlled by the abundance of initiator residues in the macroinitiator. Grafted polymer layer structure was investigated via direct interaction force measurements using colloid probe atomic force microscopy (AFM). Equilibrium, hydrated graft layer thicknesses inferred from the highly repulsive AFM force data suggest that the polymer brush graft layer contained polymer chains which were fully stretched. Since the degree of stretching resulted in layer thicknesses approaching the polymer contour length, the polymer brushes studied must be very close to maximum graft density. Grafted layers where the polymer molecules were in the mushroom regime resulted in much thinner layers but the chains had greater chain entropic freedom as indicated by strongly attractive bridging interactions between tethered chains and the silica colloid probe. Use of this experimental methodology would be suitable for preparing grafted polymer layers of a preferred density free from substrate-specific linking chemistries.

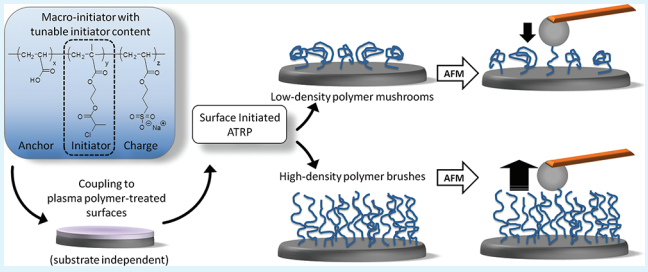

KEYWORDS: *biomaterial interface engineering, surface-initiated ATRP, polymer brush, colloid probe microscopy, plasma polymerization, biomaterial surfaces*

INTRODUCTION

Surface-initiated atom transfer radical polymerization (SI-ATRP) continues to be a popular and versatile method for surface modification of materials, allowing polymer chains to be grown from surfaces with excellent control over the molecular weight and polydispersity.[1−5] It is also an attractive method for decorating surfaces with "brushes" composed of polymer chains − a fascinating class of materials because of their unique properties for conferring resistance to protein fouling,[6] for controlling cell adhesion,[7] as new chromatographic[8−10] and filtration media,[11] and as bioactive surface coatings.[3,4]

A polymer brush can be defined as an arrangement of polymer chains terminally attached to a surface with a distance between the chains, *s*, such that *s* is less than twice the radius of gyration (*Rg*) of the polymer.[12] Practically speaking, grafted chains will stretch away from the surface due to an entropic penalty suffered from surface crowding and come to equilibrium in a extended conformation, which is defined as the equilibrium layer thickness.[13] Compared to grafting regimes that do not satisfy the brush condition (e.g., "mushroom" conformation), fabrication of true polymer brush layers is aided in part from design principals promoting high graft surface densities (or low values of *s*). Both high and low density brushes are useful in different application areas. Fabrication of high-density polymer brushes may be useful for providing an entropic barrier preventing adsorption to the surface.[7,14] However, low density polymer brushes allow for a greater degree of post polymerization modification when used as a conjugation platform[15] also exemplified for potential biosensors.[16] Therefore, it may well be beneficial to develop surface modification strategies that allow for incorporation of a desired number of surface initiators for the purpose of tuning the graft density. Since grafting of low-polydispersity chains with a tunable molecular weight is readily achieved through SI-ATRP, surface modification promoting control over *s* is a critical yet difficult parameter to modulate in a controlled way.

Received: March 15, 2012
Accepted: April 19, 2012
Published: April 19, 2012

Scheme 1. Synthesis of PolyATRP Initiator (PATRPI)

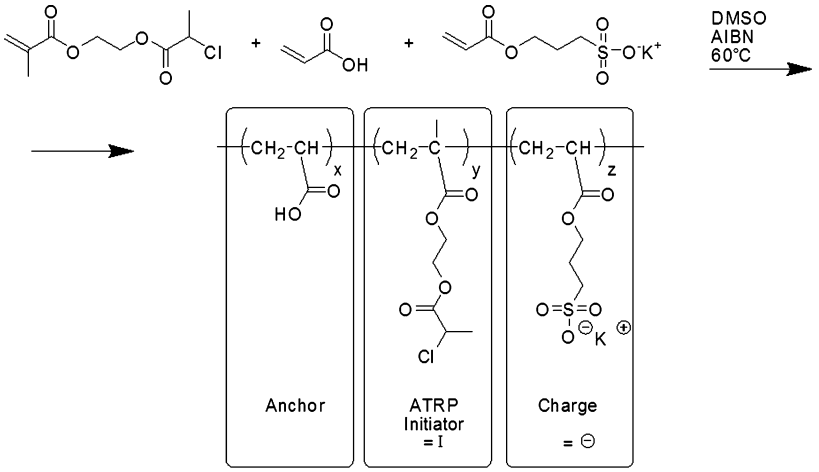

1
Poly ATRP initiator
PATRPI

Direct evaluation of the equilibrium layer thickness of the grafted polymer chains arising from different initiator densities can be measured in situ and in a hydrated state using relevant analytical techniques. Atomic force microscopy (AFM) has been useful in this regard because fundamental work has yielded methods for nondestructively interrogating the polymer surface with a spherical surface probe to extract force data that can be correlated directly to physical properties of the polymer brush.[17−22] Thus, to gain control over and understand the surface properties of a polymer brush, it is essential to have methods for controlling the polymer graft density and molecular weight, paired with methods for nondestructively probing the characteristics of the surface layers.

Methods to control graft density in SI-ATRP include an empirical approach, by manipulating reagent concentrations affecting polymerization[23,24] or postpolymerization cleavage of polymer chains from a labile anchor point using partial hydrolysis[14,23,25,26] or photodecomposition.[18] A more intuitive method is to invoke surface design choices before grafting to provide a platform where the number of potential initiation sites can be controlled. All have certain advantages; however, it is this last strategy that arguably is the most practical. Gold and silicon surfaces have been instructive here and methods such as vapor phase deposition,[27−29] electrochemical potential,[30] mixed silanes,[31] self-assembled monolayers[32] using a Langmuir−Blodgett apparatus,[33] and photodecomposition[18] present ways of tuning the initiator content on these surfaces. However, the nature and expense of gold surfaces, the toxicity and reactivity of reagents and organic solvents used to accomplish coupling (particularly on silicon surfaces), and possible instability of the grafted layer in biologically relevant conditions[31] may not be suitable for biomedical applications.

Another way to functionalize surfaces with different quantities of initiating groups is to covalently graft onto the surface a compound containing a defined amount of initiator moieties. Macroinitiators, as defined in this work, are large, compound molecules composed of both initiating and anchoring moieties. Because the amount of initiator moieties in purified macroinitiators can be quantified in solution by NMR, there is an opportunity to immobilize these and thus tune the surface initiator content. Surface linking is facilitated by adsorption or covalent linking to complementary surface functional groups. The focus of a recent SI-ATRP review, polyelectrolyte macro-initiators are particularly well suited to charged surfaces which are difficult to derivatize by chemical means.[34] Not limited to charged surfaces, one example given for polymeric surfaces showed how a photo reactive anchoring group allowed macro-initiator coupling to polymeric surfaces for SI-ATRP.[35]

For all initiating surfaces described so far, preparation of density-variable materials has, in some way, depended upon the nature of the chemical groups present on the surface. Using established methods, it is therefore difficult to develop a cross-platform method for manufacturing identical surface coatings for all types of bulk materials that could be potentially useful biomaterials.

We have previously described a technology where application of a plasma polymer thin film facilitates the substrate-independent covalent anchoring of macroinitiators (ATRP, RAFT, iniferter) to the surface, allowing for controlled radical polymerization which results in homogeneously grafted materials.[36] Recently, we have shown how this technology (with SI-ATRP) can be used to create the same protein-resistant surface coatings on a variety of different bulk materials (organic, inorganic, hard, and soft).[37]

In the present study, we control the density of polyethylene glycol methyl ether methacrylate (MW ∼ 475) (PEGMA) polymer graft layers and provide examples of two extremes where the graft layers contain polymer molecules in either the "mushroom" or "brush" conformation. This is possible because the mole fraction of initiator moieties in the macroinitiator (low or high) can be easily tuned in a representative way according to the feed concentrations used during synthesis. The macroinitiator is one component in a novel method where substrate-specific linking chemistries are largely irrelevant thus permitting any surface to be decorated with grafted layers of variable density. The macroinitiator used is a terpolymer consisting of carboxylic acid residues, α-chloroester moieties, and sulfonic acid residues. This last moiety confers a local negative surface charge − an important consideration for SI-ATRP.[38] We used AFM force measurements with a colloid probe to evaluate the polymer graft layers formed, infer structural information, and measure the equilibrium layer thickness of the grafted chains in the hydrated state. Finally,

Scheme 2. Surface Modification Scheme for Initiator Functionalization and Polymer Grafting

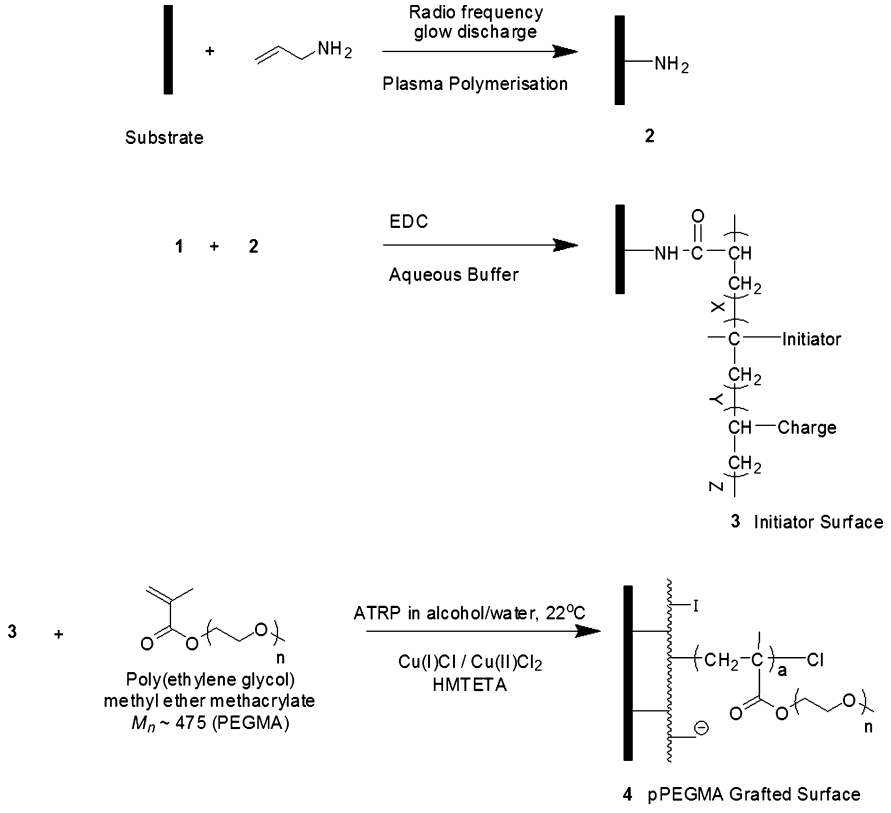

pPEGMA brushes were grafted from the surface of plastic cell culture plates in order to fabricate non cell-adherent surfaces. These approaches demonstrate greater versatility for SI-ATRP – particularly to the manufacture and characterization of surface functionalized biomaterials.

EXPERIMENTAL SECTION

General. Square silicon wafers were cut from 100 mm diameter wafer disks MMRC PTY LTD (VIC, Australia). Tissue culture polystyrene plates (TCPS, 96 well flat bottom) were purchased from BD (NSW, Australia). Allylamine (99%), dichloromethane (>99.5%), 2-chloropropionyl chloride (97%), 2-hydroxyethyl methacrylate (97%), triethylamine (>99%), 3-sulfopropyl acrylate, potassium salt (98%), poly(ethylene glycol) methyl ether methacrylate (average MW ~ 475), 1, 1, 4, 7, 10, 10-hexamethyltriethylenetetramine (HMTETA, 97%), *N*-(3-dimethylaminopropyl)-*N*′-ethylcarbodiimide (EDC, ≥97%), and inhibitor-remover were obtained from Sigma-Aldrich. Ethylenediamine-tetraacetic acid disodium salt (Na_2EDTA, 99%) was obtained from BDH, Australia. Copper(II) chloride (≥98%) and sodium chloride were obtained from Merck Pty. Copper(I) chloride was purchased from Ajax Finechem, New Zealand. Dialysis membrane tubing (MWCO: 6–8000) was purchased from Spectra/Por, USA. Acrylic acid (≥99.0%) was purchased from Fluka and was distilled prior to use. All water used was purified through a Milli-Q Gradient purified water system (Millipore Australia Pty) and had a resistivity of 18.2 MΩ cm. Phosphate-buffered saline, (PBS, pH 7.2) solution was prepared from BupHTM packages obtained from Thermo Scientific, USA prepared in Milli-Q water. RBS-35 detergent concentrate was purchased from Thermo Scientific, USA.

Initiator Synthesis. Poly ATRP initiator (hereafter referred to as PATRPI) is an ATRP macroinitiator terpolymer synthesized by varying the concentration of monomers in the feed. The following method describes an example for synthesis of a high-initiator composition terpolymer (see Scheme 1). First, the polymerizable ATRP initiator monomer 2-(2-chloropropanoyloxy)ethyl methacrylate was synthesized as previously described.[37] Acrylic acid (1.1 g) was passed through a 6 mL column of inhibitor remover followed by 10 mL of DMSO. An 0.89 g sample of 2-(2-chloropropanoyloxy)ethyl methacrylate, 0.24 g of 3-sulfopropyl acrylate, potassium salt, and 0.067 g of azobisisobutyronitrile (AIBN) was added to the DMSO/acrylic acid solution. This solution was deoxygenated at room temperature by purging N_2 for 30 min. The polymerization was initiated by heating to 60 °C and stirring for 18 h in an incubator. The resulting solution was placed in dialysis tubing (MWCO 6–8000) and dialyzed against water for at least three days with daily solvent changes. Excess water was removed by evaporation under reduced pressure. The terpolymer composition was analyzed by ^{13}C NMR to determine the proportion of each monomer residue (^{13}C NMR (in DMF + $Cr(acac)_3$ in DMF-H_7 + DMSO–D_6, 25 °C, 500 MHz). From replicate synthesis, the following peaks were found to be sensitive indicators for monomer residue composition. Carboxylic acid residue {δ = 178.64 (1C)}; 2-(2-chloropropanoyloxy)ethyl methacrylate residue {δ = 171.05 (1C), 63.76 (2C), 20.97(1C)}; 2-sulfopropyl acrylate residue {δ = 66.36 (1C), 47.59 (1C), 23.39 (1C)}. Peaks areas in a set were normalized by number of carbons and averaged.

Substrate Preparation. Silicon wafer substrates were cut from the wafer using a glass cutter into approximately 0.7 cm squares and cleaned by sonicating in 2% RBS water solution for 30 min then rinsing several times with water and ethanol, and drying with purified nitrogen. Before use, substrates were treated for 30 min by UV/ozone treatment in a ProCleaner instrument from Bioforce Nanoscience, USA.

Plasma Polymerization. The substrate surfaces were prepared using allylamine vapor and radio frequency glow discharge (RFGD) techniques to deposit a cross-linked, organic thin film with amine functionality (product **2** in Scheme 2). The radio frequency field was generated in a custom-built reactor.[39] The parameters chosen for the RFGD deposition of allylamine films were a frequency of 200 kHz, a load power of 20 W. The initial pressure of the reactor was 0.150 Torr and the treatment time was 25 s.

Surface Initiator Coupling. Covalent coupling of the ATRP initiator terpolymer to the substrate surfaces (product **3** in Scheme 2) was carried out as follows. PATRPI solutions of 1 mg mL^{-1} were prepared in PBS buffer. The coupling ratio of EDC to carboxylic acid residues was maintained at a molar ratio of 1.2:1. For the terpolymer described above, EDC was added to the solution above at a concentration of 1.5 mg mL^{-1}. Immediately after the allylamine RFGD thin film deposition, substrates were immersed into the coupling solution and placed on a gently agitating platform for 4 h at room temperature. Substrates were washed extensively with Milli-Q water to remove any noncovalently attached initiator.

Synthesis of the Grafted Layers. Initiator-coupled surfaces were then grafted with PEGMA by SI-ATRP (product **4** in Scheme 2). The ATRP catalyst system was composed of activating and deactivating copper catalysts (Cu(I)Cl and $Cu(II)Cl_2$, respectively), with 1,1,4,7,10,10-hexamethyltriethylenetetramine (HMTETA) as the chelating ligand. The molar proportions of monomer:CuCl:-$CuCl_2$:HMTETA were 20:1:0.2:2. The reaction was scaled to 1.2 mL with 70:30 mixtures (v/v) of alcohol (either ethanol or methanol) to water. Monomer concentrations were varied in the range of 0.2 to 1.0 M.

Alcohol/water mixtures and PEGMA were deoxygenated by nitrogen bubbling for 1 h. PEGMA was used as supplied as it was found that the inhibitors did not interfere with the polymerization. The catalyst system was purged in a nitrogen atmosphere for 15 min before use. SI-ATRP took place on PATRPI-silicon substrates placed in a 24 well plate with monomer and catalyst on a gently shaking platform in a nitrogen-filled glovebox for 24 h at room temperature.

Post reaction, the solutions were exposed to air to quench the reaction. The substrates were washed with water, 50 mM Na_2EDTA, and 50 mM $NaHSO_3$ solutions. Finally, substrates were exhaustively washed with water and dried under purified nitrogen. Complete removal of all traces of copper catalyst could be confirmed from an absence of copper peaks in elemental survey spectra obtained using X-ray photoelectron spectroscopy (XPS).

Grafted Cell Culture Materials. Tissue culture polystyrene 96 well plates were treated with allylamine plasma polymer. To each well was added 150 μL of PATRPI (high-initiator composition)/EDC solution. Samples were incubated and washed as above. For SI-ATRP, conditions were used as above with ethanol/water as the solvent and [PEGMA] = 1.0 M and a reaction volume of 100 μL.

Polymer Characterization. Solutions were collected post polymerization and analyzed by gel permeation chromatography (GPC) for solution polymer. Samples were diluted in mobile phase (0.1 M sodium nitrate) and filtered through 0.2 μm filters before injection into a Shimadzu chromatography system (LC-20AD) pumping at 0.8 mL min^{-1}. The columns used were a 75 × 7.5 mm guard column (Bio-Rad), followed by Ultrahydrogel 2000 and 120 columns (300 × 7.8 mm, Waters Corporation) connected in series. Columns were maintained at 40 °C. The detectors used were a Dawn HELEOS II light scattering detector and an Optilab rEX refractive index detector (Wyatt Technology Corporation). Polydispersities were calculated using ASTRA V software (Wyatt Technology Corporation) and molecular weights were calculated absolutely using a value of 0.1275 mL g^{-1} for the refractive index increment determined in separate experiments with purified pPEGMA.

X-ray Photoelectron Spectroscopy. X-ray photoelectron spectroscopy (XPS) analysis was performed using an AXIS HSi spectrometer (Kratos Analytical Ltd., Manchester, UK), equipped with a monochromatic Al Kα source at a power of 144W (12 mA, 12 kV). Charging of the samples during irradiation was reduced by an internal flood gun, coupled with a magnetic immersion lens. Each sample was analyzed at an angle normal to the sample surface. Survey spectra were acquired at 320 eV pass energy and high-resolution C 1s spectra were recorded at 40 eV pass energy. Data were processed with CasaXPS software ver.2.3.13 (Casa Software Ltd.) with residuals for curve fits minimized with multiple iterations using simplex algorithms.

Colloid Probe Microscopy. The interactions between spherical silica colloid probes and pPEGMA grafted samples (prepared either in ethanol/water or methanol/water solutions) or control samples (either cleaned silicon wafer substrates or PATRPI-silicon substrates) were measured using a MFP-3D atomic force microscope (Asylum Research, Santa Barbara, CA) in phosphate buffered saline (PBS, pH 7.2, 0.15 M NaCl). The silica colloid probes were prepared by attaching a spherical silica particle (Bangs Laboratories, IN; $R \approx 2.2$ μm) onto Au coated, triangular Si_3N_4 cantilevers (DNP, Veeco Instruments, Inc., CA) using an epoxy resin (EPON 1004, Shell) and a xyz translation stage. The spring constant of these cantilevers was determined to be 0.219 ± 0.019 N/m using the resonance frequency method of Cleveland et al.[40] and the radius of the sphere was determined using optical microscopy either prior to or immediately after an experiment.

The general procedure for force measurement experiments was as follows. All surfaces which came into contact with the PBS solution (fluid cell components, cantilever holder etc) were first cleaned in a 2 vol % RBS35 surfactant solution either for 1 h in an ultrasonic bath or overnight soaking, followed by copious rinsing with ultrapure water and finally blown dry using a high velocity, filtered, purified nitrogen stream. In our case, the cantilever holder used did not contain any electronic components and could be fully immersed in aqueous solutions. The glass discs that formed the bottom of the fluid cell were cleaned immediately prior to an experiment using an UV/ozone cleaner (Bioforce Nanosciences, Ames, IA, USA) for one hour. The silica colloid probe was also cleaned immediately prior to an experiment using a custom built UV/ozone cleaner for 1 h. Samples for analysis were quickly mounted on the glass discs using an epoxy resin and fitted into the fluid cell. Samples were equilibrated in PBS solution for 20 − 30 min prior to force curve acquisition.

Data were collected as cantilever deflection versus linear variable differential transformer (LVDT) signal and converted to F/R (force scaled by the radius of the attached sphere) versus apparent separation distance using the MFP-3D software. In all cases, the data was converted using an average inverse optical lever sensitivity (InvOLS) factor obtained from repeated measurements of the voltage associated with tip deflection against a hard control surface (e.g., allylamine plasma polymer surface in PBS). The approach velocity used was below 2 μm/s in all cases, and data were collected using a relative trigger of 0.5 V. At least ten force curves were collected from five positions on each sample. For each of these data sets, large deviations from the norm were not observed, suggesting good surface homogeneity. An "average response", representative force curve for each sample was selected from each data set for comparison to other samples.

Cellular Adhesion Studies. Cell attachment and spreading on plates was investigated using L929 mouse fibroblasts (cell line ATCC−CCL-1, Rockville, MD, USA). Cells were cultured in MEM containing 10% fetal bovine serum and 1% nonessential amino acids (Gibco, Invitrogen, USA). Prior to cell studies, samples were thoroughly washed in Milli Q water and then soaked in phosphate buffered saline (PBS) containing antibiotic/antimycotic solution (Gibco, Invitrogen, USA) for 24 h at 4 °C which was subsequently removed prior to cell seeding. Experiments were conducted both in the presence and absence of fetal bovine serum. Cells were seeded at 2.5×10^4 cells/cm^2 and incubated for 22 h at 37 °C, 5% CO_2 in air. Cells were imaged at 100 times magnification using a Nikon inverted microscope (Eclipse T2000-U).

RESULTS

Synthesis of PolyATRP Macroinitiator. Two different polyATRP macroinitiators (PATRPI) were synthesized according to Scheme 1 and characterized by ^{13}C NMR. The composition of each macroinitiator could to be reliably tuned in response to the feed proportion of each of the three monomers (Table 1). In this way, initiator 2 was prepared with approximately double the ATRP initiator content (18.5% vs 10.2% by mass) as initiator 1, but with similar sulfonic acid residue content.

Table 1. Monomer Feed Composition Was Reflected in the Actual Terpolymer Composition As Measured by ^{13}C NMR[a]

	initiator 1 – low abundance ATRP initiator		initiator 2 – high abundance ATRP Initiator	
	feed mass %	^{13}C NMR mass %	feed mass %	^{13}C NMR mass %
carboxylic acid residue (X)	85.0	83.1 ± 5.0	75.2	73.6 ± 4.4
ATRP initiator residue (Y)	10.0	10.2 ± 0.6	19.8	18.5 ± 1.1
sulfonic acid residue (Z)	5.0	6.7 ± 0.4	5.0	7.9 ± 0.5

[a]Presented errors are due to instrumental and processing uncertainties.

Initiator Coupling. Results of XPS analysis following macroinitiator coupling to plasma polymer treated substrates are presented in Table 2. Compared to the allylamine plasma polymer surface, PATRPI layers partially attenuated the underlying nitrogen signal (nitrogen content was typically 10% for the allylamine plasma polymer surface). Well below the sampling depth of approximately 10 nm, the initiator formed a coating of a few nanometers thick (further characterization given below). Notably, the presence of chlorine and sulfur in the coating was verified by XPS analysis. Furthermore, when comparing XPS analysis results obtained from surface-bound initiators 1 and 2, the polymer composition was reflected in the composition of the surface, with the initiator 2 surface layer having roughly double the chlorine content of the initiator 1 surface layer and both having approximately equal sulfur content.

Table 2. Relative Elemental Surface Composition of Allylamine Plasma Polymer and PATRPI Coatings Determined by XPS

relative elemental %	allylamine plasma polymer coating	initiator 1 – low abundance ATRP initiator	initiator 2 – high abundance ATRP initiator
C	76.0	67.2	68.0
N	10.4	5.67	4.65
O	13.6	25.6	24.9
Cl	0.00	0.72	1.68
S	0.00	0.80	0.74
Si	0.00	0.00	0.00

Aqueous ATRP Grafting of pPEGMA from Flat Surfaces. For each initiator surface, the concentration of PEGMA used for SI-ATRP was varied up to 1 M in both methanol/H_2O and ethanol/H_2O solutions (70:30 v/v). These two solvents were chosen as a basis for varying the solvent polarity to observe what effect this would have on the physical properties of the grafted layer. Analysis of these grafted layers by XPS revealed characteristic changes in the elemental composition of the surfaces which would be expected for a graft pPEGMA layer (see the Supporting Information, S.I. Figure 1). Changes were also observed in the high-resolution C 1s spectra obtained for these surfaces. This is best seen in Figure 1 where example C 1s spectra are presented for the low abundance initiating surface in ethanol/H_2O solutions. As the monomer concentration was increased, the relative area of the C3 (ether) carbon component increased, suggesting increasing amounts of pPEGMA were being grafted from the surface (i.e., higher molecular weight pPEGMA chains were obtained as the [PEGMA] was increased). This trend was also observed in both solvent systems studied and for both low and high abundance initiating surfaces (see the Supporting Information, S.I. Figure 2).

After polymerization, the solution above the grafted substrates was retrieved for analysis. In these solutions, pPEGMA was characterized by GPC/MALLS and the molecular weight and polydispersity was determined (see the Supporting Information, S.I. Figure 3). Solution polymer can be formed in the absence of added sacrificial initiator when radical transfer from the surface bound initiators transfers to solution early in the polymerization.[38,41] For some reports of SI-ATRP, an agreement has been shown between properties of the solution polymer and the surface polymer,[5,23,24,37,38] although there are exceptions for some reaction conditions. The applicability of this assumption is discussed below.

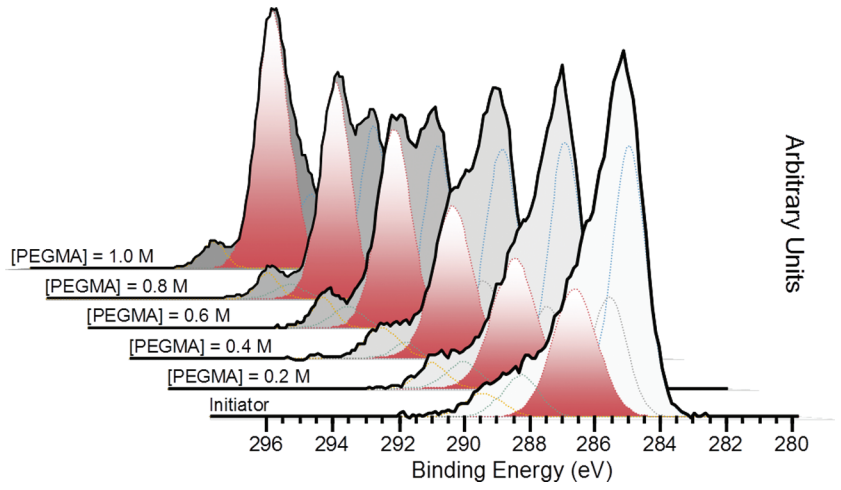

Figure 1. Overlay of high-resolution XPS C1s spectra for initiator 2 (low abundance ATRP initiator) and grafted substrates in ethanol/water solutions. The solution concentration of PEGMA monomer is given. Peak fitting (dashed, colored lines) was performed using a five-component model with Gaussian:Lorentzian (70:30) line shapes, with residuals minimized with simplex algorithms. The C3 (C–O, 286.5 eV) component is highlighted in red.

Thickness Measurements. The step height profile of a scratch through the polymer coating on silicon wafers, obtained using profilometry, provided an estimate of the dry-layer thickness relative to the hard silicon surface underneath. Graft layer thicknesses were plotted against PEGMA monomer feed concentration as shown in Figure 2. Here data are plotted for

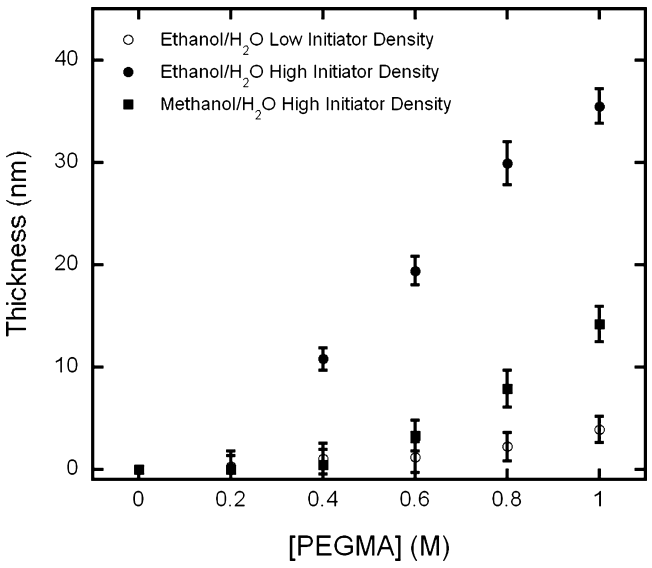

Figure 2. Graft layer thicknesses determined by profilometry for pPEGMA grafted from initiator 1 (low abundance ATRP initiator in ethanol/water mixtures, ○), and initiator 2 (high abundance ATRP initiator in ethanol/water solutions, ●; and in methanol/water solutions, ■). Reported graft thicknesses are relative to the initiator layer. Uncertainties represent one standard deviation ($n \approx 7$).

both high and low abundance initiating surfaces in ethanol/H_2O solutions and for the high abundance initiating surface in methanol/H_2O solutions illustrating both the effect on graft layer thickness of the solvent used and of the initiator layer surface density. In addition, where possible, XPS overlayer calculations provided a second method to estimate dry thickness of the pPEGMA graft layers. These are compared to the results from profilometry (see the Supporting Information, S.I. Table 1). Given the accuracy of both techniques and the assumptions made in the calculations, there was reasonable concordance between the values obtained using the two different techniques. The data obtained by profilometry for the low abundance initiating surface in methanol/H_2O solutions was not presented in Figure 2 due to uncertainty associated with the profilometry measurements for the relatively thin coatings generated, however, the results obtained from overlayer calculations suggested that the pPEGMA graft layers were lower than those obtained with the low abundance initiating surface in ethanol/H_2O solutions, in agreement with the data for the high abundance initiating surface (see the Supporting Information, S.I. Table 1).

Colloid Probe Microscopy. In these experiments, a silica sphere with a radius of approximately 2 μm was glued to the tip of an AFM cantilever and brought into contact with grafted and control surfaces in high ionic strength PBS solution. Force measurements were interpreted in relation to the allylamine plasma polymer surface, a material that behaves as an inelastic solid and allows the photodetector response to be calibrated. This measurement gives $\delta D/\delta V$ or inverse optical lever sensitivity (InvOLS) where D is the distance traveled and V is the voltage associated with deflection of the cantilever in hard wall contact. The resultant forces were finally scaled by the radius of the silica sphere. For measurements of this type, the zero separation distance is not known independently and must be inferred from the force curves themselves. For samples of the type studied here, this is generally not possible since the graft polymer layers were still being compressed at the highest loads applied during the experiment (i.e., the InvOLS measured from a force curve was never the same as for a noncompressible control surface). Hence there was always a compressed polymer layer between the silica sphere and the sample substrate at the highest loads, the thickness of which cannot be measured independently. In addition, this value is not a constant as the thickness of the pPEGMA graft layers varied with each sample analyzed and the maximum applied load was always the same. As a first approximation, the force data obtained was offset along the *x*-axis by the average dry thickness obtained from the profilometry experiments with identical samples prepared from the same batch. This is most likely an underestimate of the true hydrated thickness of the graft layers in most cases but it provides a mechanism by which the force curves can be offset for clarity in the figures and the range of the forces then provides an estimate of the hydrated thickness. The data obtained fell into two categories; (i) purely repulsive interactions and (ii) attractive interactions at large apparent separation distances followed by repulsive interactions at shorter apparent separation distances, depending on the monomer concentration, solvent system and the surface density of initiators. In Figure 3 are presented the data obtained for the pPEGMA graft layers formed using a low abundance initiating surface from both (a) ethanol/H_2O and (b) methanol/H_2O PEGMA solutions. Here it may be observed that the interactions followed category (ii). Generally speaking, the range of the strongly attractive interactions was larger in the case of the surfaces prepared in ethanol/H_2O solutions (>60 nm) compared to the surfaces formed from methanol/H_2O solutions (<55 nm). This is more readily observed in the lower figures, which present the detail in panels a and b in Figure 4. Also indicated on these figures are red arrows, indicating spring instabilities under the influence of strongly attractive forces (i.e., at the positions indicated, the surfaces jump into contact and the data obtained in this region was nonequilibrium in nature and has been removed from the figures). It may also be readily observed that for all the surfaces tested, whether the longer range interactions were attractive or repulsive, the force data at short separation distance (<40 nm) was always repulsive, indicating that the polymer layers were being compressed by the silica sphere up to the highest loads tested.

Presented in Figure 4 are the force data obtained for pPEGMA graft layers formed using the high abundance initiating surfaces in both (a) ethanol/H_2O and (b) methanol/H_2O pPEGMA solutions. The forces measured were purely repulsive in all cases (i.e., category (i) for all monomer concentrations tested and for both solvents tested). The onset of probe deflection is a measure of the equilibrium layer thickness of the polymer grafts in solution and these values are give in Table 3. Generally speaking, the range of the interactions obtained for pPEGMA graft layer surfaces formed in ethanol/H_2O solutions were larger than for those formed in methanol/H_2O pPEGMA solutions, suggesting that the pPEGMA graft layers were thicker. The increasing magnitude of this force at a given distance was related to the increasing

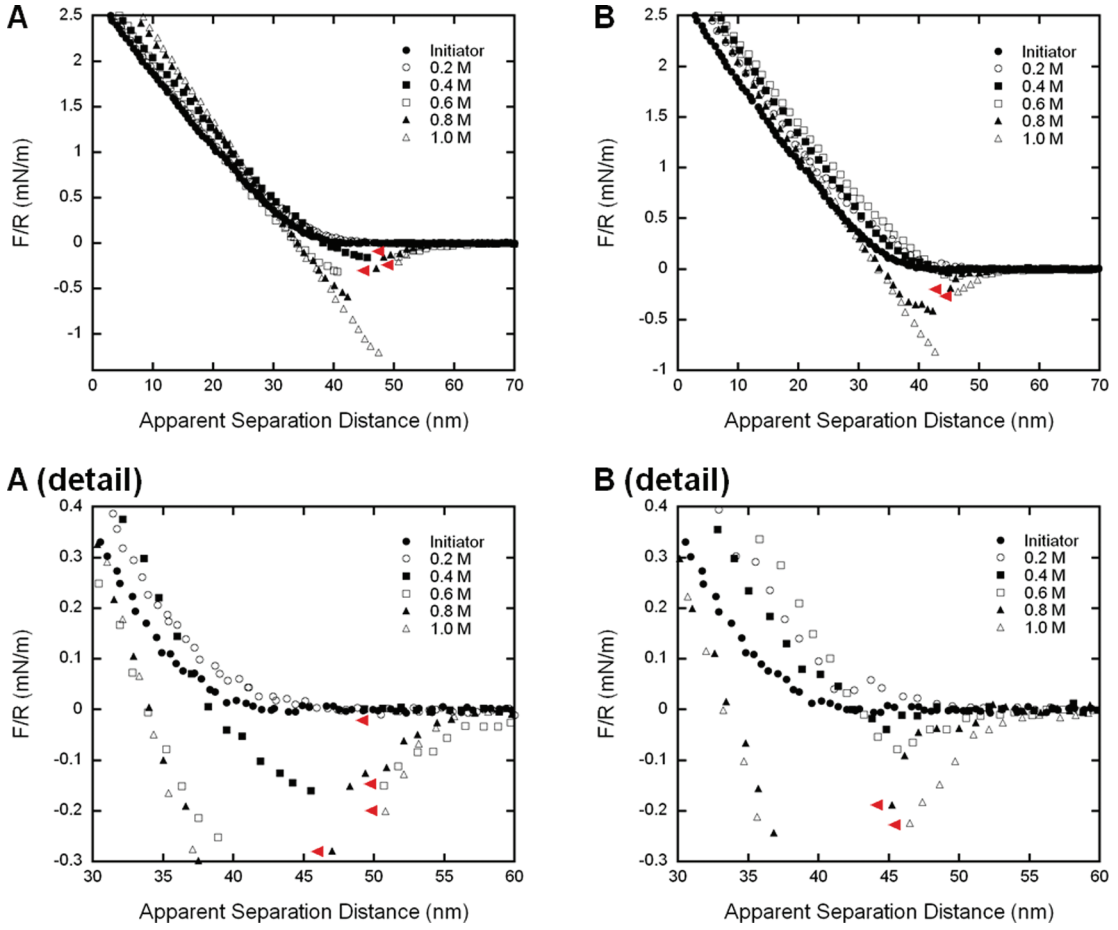

Figure 3. Representative AFM force compression curves for colloid probe approaches to control and grafted surfaces using initiator 1 (low abundance ATRP initiator). The concentration of PEGMA used for polymerization is given in the legend. (A) Ethanol/water polymerization solvent. (B) Methanol/water polymerization solvent. Detail (zoomed areas) are shown. Red triangle markers indicate positions of data discontinuity where strongly attractive forces have resulted in a jump to contact between the AFM probe and the grafted surface.

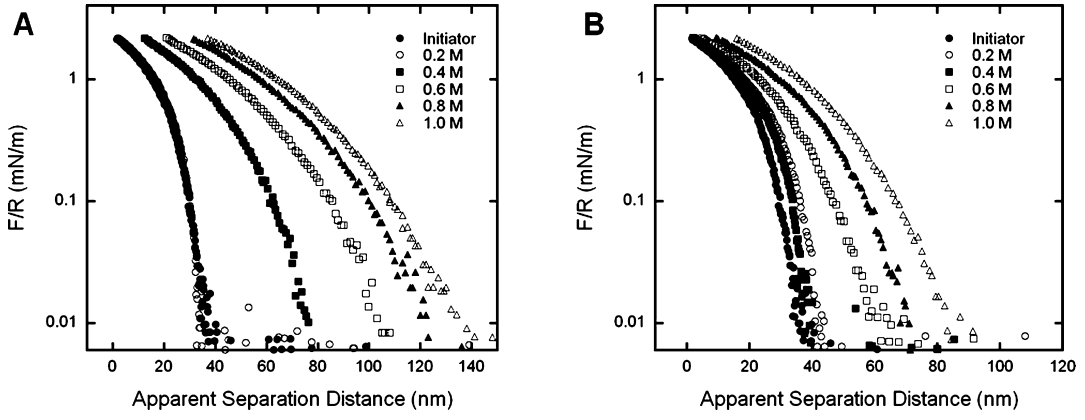

Figure 4. Representative AFM force compression curves for colloid probe approaches to control and grafted surfaces using initiator 2 (high abundance ATRP initiator). The concentration of PEGMA used for polymerization is given in the legend. (A) Ethanol/water polymerization solvent. (B) Methanol/water polymerization solvent. The apparent separation distance has been offset by the measured dry thickness.

concentration of PEGMA used in the SI-ATRP suggesting molecular weight effects. Differences in compressibility for initiator 1 and 2 grafted surfaces suggest differences in grafting density.

Cellular Adhesion Studies. The attachment of L929 cells to control and modified surfaces was studied to see what effect the graft coating had on cell adhesion and spreading. Different cell morphologies were observed depending upon cellular exposure to the uncoated (TCPS) surface, the initiator modified surface (PATRPI), or the grafted surface (pPEGMA). Presented in Figure 5 are images of cells on surfaces after 22 h incubation with FBS present in the cell culture medium. On the initiator sample, we observed less cell binding and spreading compared to the TCPS control. On the pPEGMA grafted

dx.doi.org/10.1021/am300463q | ACS Appl. Mater. Interfaces 2012, 4, 2811−2823

Table 3. Graft Polymer Equilibrium Layer Height (H) Measured by Colloid Probe Microscopy for pPEGMA Chains on High Abundance ATRP Initiator Surfaces[a]

	H (nm)	
[PEGMA] (M)	ethanol/H_2O	methanol/H_2O
0.2	4.7 ± 0.5	6.3 ± 0.4
0.4	52.4 ± 2.8	10.1 ± 0.8
0.6	71.1 ± 4.3	26.7 ± 1.7
0.8	91.1 ± 8.7	45.6 ± 3.8
1.0	107 ± 7.3	54.8 ± 3.4

[a]The layer height is the average value expressed relative to the initiator. Uncertainties represent one standard deviation ($n \approx 20$).

sample, cells did not attach or spread on the grafted layer. Instead, cells self-associated into clusters. These clusters settled on the surface but became detached with gentle shaking. The presence of FBS did not influence the adhesion as FBS-negative samples showed similar results (data not shown).

DISCUSSION

We have grafted pPEGMA from initiator-functionalized surfaces at different grafting densities responding to the design properties of a novel macroinitiator. The grafting methodology makes use of a platform technology recently described allowing many different surfaces to be functionalized with ATRP initiators and then grafted with polymer brushes whose grafted lengths could be easily manipulated.[37] In this previous work we described the protein resistance of polymer-grafted films produced from many different substrates in response to the thickness of the polymer brush layer. From this and the work of others, it is clear that changing the thickness of the coating is one way in which to improve the biocompatibility of grafted substrates.[14,22,42,43] Another important way is to manipulate the grafting density thereby providing a steric barrier to protein adsorption and cellular adhesion.[44] This is more difficult to achieve in surface-initiated polymerizations because methods must be developed to provide a surface with a variable surface density of initiators from which to graft. In the work that we describe below, we build on our previous investigation with immobilized macroinitiators and show how using macroinitiators of variable composition allow variable-density surfaces to be created.

Controlling Initiator Surface Content. The initiator surface content was manipulated by changing the proportion of ATRP moieties in a macroinitiator and then coupling it to a plasma polymer treated surface. For this, we synthesized a new ATRP macroinitiator terpolymer consisting of different monomer units to act as anchors, ATRP initiators, and charged groups (Scheme 1). Use of charged groups has two advantages. First, the macroinitiator was soluble in water. Thus the substrate-independent coupling technique can proceed in buffer solution and would allow for functionalization of a wider range of polymeric surfaces (e.g., some plastic cell culture ware that is incompatible with organic solvents). Another advantage is the presence of a strong anionic surface group. It is hypothesized that anionic groups such as sulfonic acid facilitate surface initiated ATRP by accumulating positively charged Cu(I) at the surface near ATRP initiators.[45] This allowed better comparison with previous experimental work on SI-ATRP from sulfonated surfaces.[23,24,38,45−47]

The quantity of the ATRP component in the macroinitiator matched the monomer feed concentration congruently. This enabled the synthesis of macroinitiators with both low and high initiator content. We hypothesized that these proportions would span a range of initiator concentrations that when immobilized on the surface could produce potentially high variability in graft density and therefore, produce grafted surfaces with widely different physical properties.

Finally, the proportion of sulfonic acid residues was designed to remain approximately constant. This allowed the quantity of ATRP moieties to be always proportionally larger than the charged moieties by factors roughly equal to 2 and 4 times in initiators 1 and 2, respectively. ^{13}C NMR data revealed that the final monomer residue proportions in the polyATRP initiator were representative of the intended design (Table 1), suggesting a way of reliably tuning the macroinitiator composition to intention.

Surface coupling of the macroinitiator proceeded according to Scheme 2. We previously used this surface modification procedure as a way of grafting from surfaces in a substrate-independent fashion.[37] In the present work, we have grafted from flat silicon wafers as well as inside the wells of plastic multiwell cell culture plates. Surface characterization was accomplished by XPS (Table 2) and profilometry (Figure 2). More detailed XPS and thickness data is also provided in the Supporting Information. In the dry state, immobilized PATRPI formed layers measured by profilometry to be approximately 1.6 nm thick on top of the amine-rich allylamine plasma polymer film which was typically 25 nm throughout this work. The approximately double ATRP residue proportion in initiator 2 compared to initiator 1 was verified by observing the doubling of the elemental chlorine signal from XPS survey data (Cl = 1.68% and Cl = 0.72%, respectively, as shown in Table 2).

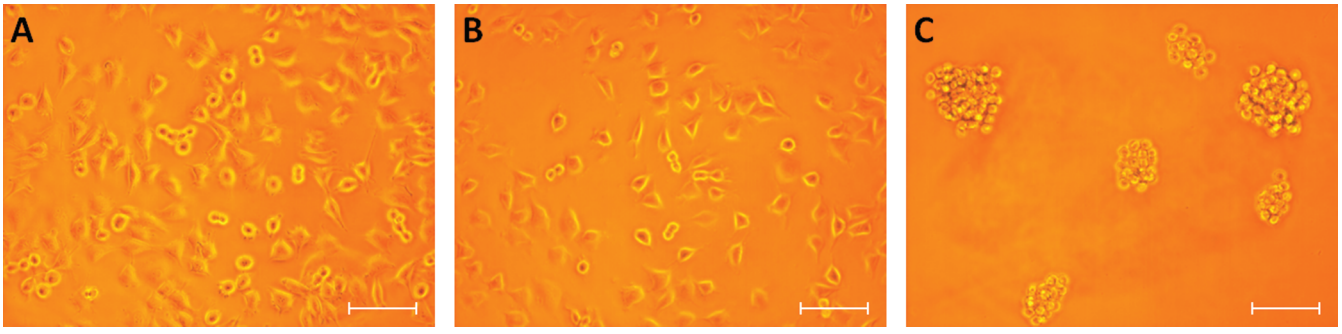

Figure 5. L929 cellular adhesion on control and modified surfaces in 96 well cell culture plates. 100 times magnification. Scale bar represents 100 μm. (A) Unmodified TCPS surface. (B) Initiator-modified surface. (C) pPEGMA grafted surface.

Furthermore the surface sulfur content was also determined to be approximately equal, as it was in the free polymer. Thus, the ATRP initiator and sulfonic acid content selected for in the macroinitiator synthesis were well represented in the final surface composition.

When probed in the hydrated state with colloid probe microscopy, the initiator layer was found to be swollen with buffer producing a repulsive force whose onset was measured at approximately 36 nm separation distance (Figure 4). On the basis of our previous observations with immobilized polymers composed of poly(acrylic acid), we would expect that the polymer chain would be pinned to the surface at positions along the backbone, which would allow loops or tails to maintain conformational freedom when hydrated.[19] The measured dry and hydrated thicknesses in the present report compare favorably to observations from this previous report.

Controlled SI-ATRP of PEGMA. Previously, we have shown living/controlled polymerization for linear polymers by SI-ATRP in water based on a the same initiator immobilization strategy and similar macroinitiator.[37] In the present work, bottle-brush type polymers were grafted from surfaces using a new macroinitiator in alcohol/water solutions. Figure 2 shows that the thickness of these pPEGMA graft layer at higher [PEGMA] increased linearly in response to increasing monomer feed concentration implying that we were able to obtain control for this system. At low [PEGMA], measured dry thicknesses were somewhat lower than what would be expected. This is more notable for polymerization in methanol/water solution and when the initiator quantity on the surface was low. We have observed that our macroinitiator forms a polymer layer that is approximately 1.6 nm in the dry state but swells to approximately 36 nm when buffer is present. Since initiators are distributed throughout this layer, after SI-ATRP, small MW chains would also form within the hydrated layer as well as at the interface. Therefore, when these layers were dehydrated and measured with profilometry, for the lowest monomer concentration samples, the polymer chains would be collapsed within the initiator layer and the observed dry thickness would not be as thick as if chains were grafted from a flat interface. During polymerizations with higher [PEGMA], longer chains result whose growing chain ends are long enough to escape the hydrated initiator layer. The measured profilometric thicknesses are similar to grafting from a flat surface and show a linear trend. The different solvent systems could have two effects. First, the degree of swelling of the initiator layer will be different and second, the ATRP reaction mechanism will be altered. We further discuss these factors below and in the Supporting Information.

XPS data showed that high-resolution C 1s peaks on full-thickness samples were characteristic of pPEGMA containing near theoretical peak areas of modeled components (see Figure 1 and the Supporting Information, S.I. Figure 2, for more detailed analysis). In particular, the thickest layers had C3/C peak ratios indicative of ether carbons close to the theoretical maximum of approximately 80% expected of the monomer. This was observed for 0.4 to 1.0 M concentrations from initiator 2 samples. For samples with pPEGMA coatings thinner than the XPS sampling depth of 10 nm (as was the case for all samples grafted from the initiator 1 surface), the resultant spectra also contained contributions from both the underlying initiator layer and the plasma polymer layer. As the grafted layer became thicker, more of the pPEGMA coating was represented in the XPS C 1s trace as shown.

Colloid Probe Microscopy. The forces observed when a silica sphere was brought near grafted and control surfaces were diagnostic of the local chain grafting environment for fully hydrated layers. Grafted surfaces produced by either initiator showed very different force profiles depending upon the abundance of ATRP initiator and the solvent in which polymerization took place. Each factor is discussed with its relationship to the equilibrium brush thickness properties of the surface grafted chains.

Low-Graft Density Surfaces. The first data set concerned the low abundance ATRP initiator: Initiator 1 (Figure 3). The force was purely repulsive for the initiator control surface. Similar phenomena was observed for colloid probe microscopy experiments for covalently immobilized poly(acrylic acid) on flat surfaces.[19] Sufficient ionic strength present in the measuring fluid effectively screened electrostatic interactions between the negatively charged sphere and surface, and so the repulsive force was due to compression of the initiator polymer layer by the silica sphere on approach. Short pPEGMA chains (0.2 M PEGMA feed concentration) had a similar force profile to the initiator layer indicating that there was little or no bridging affinity for the chains toward the probe and that the pPEGMA graft layer was very thin (i.e., the molecular weight of the pPEGMA chains was very and there were very few chains the protruded from the initiator layer). The dry layer thickness relative to the plasma polymer layer for the initiator was 1.5 ± 1.6 nm, whereas pPEGMA chains formed from the 0.2 M PEGMA solution plus the initiator layer equaled 1.8 ± 1.6 nm. Here the dry thickness of the polymer layer was virtually indistinguishable from the initiator layer, within error, suggesting that there were very few, if any, chains that protruded from the fully hydrated initiator layer as was suggested above.

End-grafted pPEGMA chains have an affinity for silica colloid probes and, if they have sufficient entropic freedom, will extend to bridge the gap between the incoming probe and the polymer graft layer, generating an attractive force.[22] The mechanism of this force has been discussed at length in previous work[22] and will not be replicated here. These attractive bridging forces were observed at [PEGMA] greater than 0.2 M. When the grafted chains had a higher molecular weight (e.g., [PEGMA] = 0.4 M), the affinity of pPEGMA chains for the colloid tip produced an attractive bridging force. For longer chains (0.6, 0.8, and 1.0 M feed concentration) the force of attraction became greater because of a greater restoring force from the grafted polymer chains. Attractive forces of this type have also been observed between end grafted polymer layers and silicon nitride AFM tips but for graft polymer layers of very different chemistry.[20] What is critical for generation of these types of forces is that the chains have sufficient entropic freedom and that there is a positive energy of adsorption for the polymer chains on silica surfaces.

Probing the hydrated polymer layers by colloid probe microscopy showed that attractive interactions (snap-to distances) were observed at a greater distance from the surface when polymerization was performed in ethanol/water mixtures compared to methanol/water mixtures (Figure 3A compared to Figure 3B). That the chains grown in ethanol/water mixtures were longer than in methanol/water mixtures was also seen from the thicker layers measured by profilometry or overlayer calculations. Longer chains are expected to extend to slightly longer distances from the surface and have more entropic

freedom allowing them to produce chain-probe bridging interactions measured at larger distances from the surface.

To summarize, polymer chains grafted from initiator 1 surfaces must have had sufficient entropic freedom to stretch away from the surface anchor to form attractive bridging forces with the colloid probe. This implies that unperturbed polymer chains would tend to exist in a low-graft density morphology (e.g., mushroom conformation).

High-Graft Density Surfaces. The forces associated with a colloid probe approaching grafted surfaces prepared from initiator 2 were all purely repulsive in nature (Figure 4). Similar observations for colloid probes[22] and AFM tips[20] have been attributed to grafted layers having polymer chains extended and stretched to such a degree that attractive bridging forces, on average, are not observed. This implies that the polymer chains are in an extended conformation due to steric crowding between nearest neighbors and exist in high-graft density ("brush") morphology.

The onset of observed repulsive force during probe approach is a measure of the equilibrium layer thickness and, therefore, certain information about the conformation of grafted chains can be ascertained. These thicknesses were estimated and are presented in Table 3. With knowledge of the properties of the graft polymer and the solution polymer from GPC, we conclude by continuing this discussion in light of the SI-ATRP mechanism under the influence of different solvents.

SI-ATRP of PEGMA in Alcohol/Water Mixtures. For polymerization of PEGMA, the properties of the solvent have been shown to be a critical factor influencing ATRP.[48−51] For our surface initiator, the observed grafted layer thicknesses clearly indicated that longer polymer chains were grown in the presence of ethanol/water solutions compared to methanol/water solutions and that these thicknesses increased with [PEGMA] (Figure 2). Due to the small surface-area of the samples used in this experiment, it was not possible to independently verify this by cleaving grafted chains in sufficient quantity to be analyzed by GPC. Thus we have relied on other methods to characterize the grafted polymer chains. We mentioned earlier that the characteristics of the solution polymer sometimes directly mirrors the characteristics of the surface polymer; however, others have shown with bottle-brush polymers like the acrylamide analogue of pPEGMA that there was a rather poor correlation at least when water was used as the solvent.[42] Therefore, we should demonstrate whether or not this is the case for our polymerizations in alcohol/water solutions. We have noticed that an overlay of the solution polymer M_n data with the measured profilometric thickness data show a similar trend suggesting an association (Figure 6). Although this is an unconventional representation of these two data sets given that we superimposed molecular weight and thickness data at different scales which we have done so for two reasons. First, it highlights the noncolinearity of points at [PEGMA] = 0.2 M which deviate from either data set trend in opposite directions. This hints of a complex initiation mechanism leading to charge transfer − the possibility of which we discuss further in the Supporting Information. Second, if the data sets were truly correlated (at least for [PEGMA] > 0.2 M), then it seems that solution polymer and surface polymer grew at the same rate with the grafting density on the surface being constant.

We can look at this data another way because our measurement from colloid probe microscopy provides another measure of the grafted layer thickness when fully hydrated. If

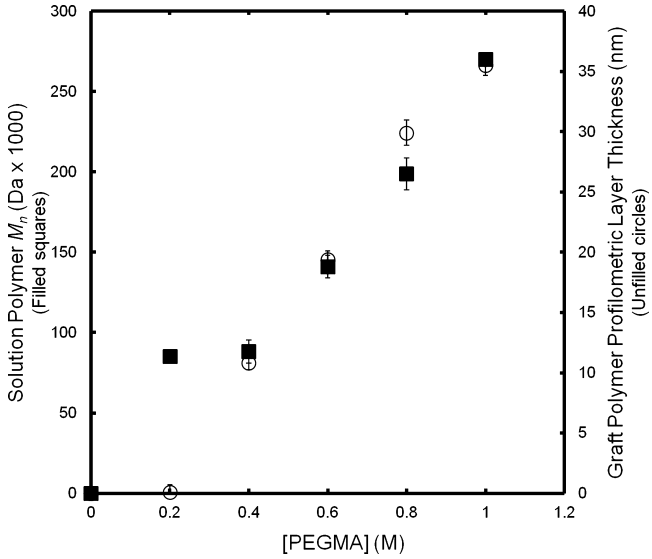

Figure 6. Molecular weight of the solution polymer (■) and the polymer layer thickness measured by profilometry (○) plotted together against the concentration of PEGMA used in the polymerization solution. Data are from high abundance ATRP initiator samples when ethanol/water was used as the solvent for polymerization. Thicknesses are relative to the initiator layer. Uncertainties in M_n are from instrumental and processing error. Uncertainties in profilometric thickness represent one standard deviation ($n \approx 7$).

we assume that the graft density was constant and resulted in maximum chain stretching, and we assume that the molecular weight of the polymer formed on the surface was identical to the solution, we can transform the solution polymer molecular weight data into a hydrated thickness to compare with the AFM data. To do this, we stretch the polymer to its contour length and measure the total length of the chain as l = 0.25DP. When tethered to the surface by one end, this would represent a polymer layer thickness calculated from the DP (degree of polymerization) and 0.25 nm, which is the length for each monomer unit in the polymer backbone projected normal to the surface based on in-plane tetrahedral geometry. This contour length is plotted along with the measured equilibrium layer thickness from colloid probe microscopy in Figure 7. Here, the data show good correlation, suggesting that the layer thicknesses that we measured with the colloid probe represent grafted polymers that were so densely packed they were forced to stretch to their contour length. Small differences in thickness between these two data sets could result from the fact that surface grafted chains were not strictly monodisperse. The agreement between the data allows for the plausible assumption that the solution polymer obtained (except where noted) was a good measure of the surface polymer M_n.

Knowledge of the graft polymer M_n permits calculation of graft density. When only the dry thickness is known, one way to estimate graft density (σ) is from

$$\sigma = \frac{T\rho N_A}{MN_b} \tag{2}$$

where T is the dry polymer thickness, and ρ is the bulk polymer density (assumed for pPEGMA to be 1.0 g cm^{-3}), M is the molecular weight of the monomer repeat unit and N_b is the number of backbone repeat units.

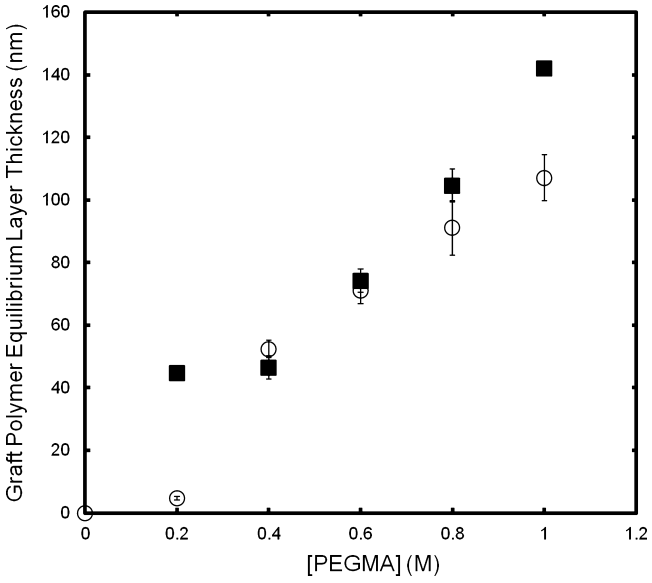

Figure 7. Comparison of the predicted polymer contour lengths for a fully stretched polymer chain (■) and the measured equilibrium layer thickness by colloid probe microscopy (○). Data are from high abundance ATRP initiator samples when ethanol/water was used as the solvent for polymerization. Contour lengths were calculated assuming that the MW of the surface polymer was identical to the solution polymer. The measured thicknesses of the grafted layers are expressed relative to the initiator layer. Uncertainties from values derived from GPC data are from instrumental and processing sources. Uncertainties from values derived from AFM data represent one standard deviation ($n \approx 20$).

Recently, work of de Vos et al. provided a model for bottle brushes based on a self-consistent field theory.[52] Here a scaling law was developed giving

$$H = K\sigma^{1/3}N^{*2/3}N_b \quad (3)$$

where H is the thickness of the polymer brush in a good solvent and N^* is a ratio accounting for the number of repeat units in the side chains and the degree of branching (a constant value for a given monomer). In this equation, we have included a constant K that allows the scaling law to be treated as an equality. For experiments such as ours when the brush height is measured in solution, the stretching of the polymer chain becomes a much more sensitive determinant for computing graft density (i.e., through the use of eq 3) because $\sigma \sim (H/N_b)^3$ compared to when the graft density is computed by the dry layer thickness (i.e., in eq 2 where $\sigma \sim T/N_b$) where the "dry" chains have packed into a homogeneous bulk material with assumed density ρ. Although it is not possible to evaluate expression 3 without knowing K our experimental data suggest that an estimate can be obtained through calculation since σ must be equal in eqs 2 and 3 and we have measured T, H and assume that N_b of the graft polymer is the same as the solution polymer. For this we have determined $K = 0.106$ which is valid for pPEGMA where thicknesses are measured in nanometers. It is clear from Figure 7 that [PEGMA] = 0.4 and 0.6 M produced brushes at maximum graft density so we obtain an average from these points giving 0.22 chains/nm^2. We discuss this calculation and discuss the suitability of using this model for our experimental work in the Supporting Information.

Ohno et al. have calculated a value of 0.18 chains nm^{-2} for PEGMA (MW ~ 475) surface grafting.[35] Feng et al. showed a maximum graft density of 0.29 chains nm^{-2} for pPEGMA chains with a smaller molecular weight (300 g mol^{-1}) in which case it would be reasonable that a higher graft density would result.[48] Finally Kizhakkedathu et al. found a maximum density of 0.52 chains nm^{-2} for PEG acrylamide (MW ~ 350) on curved latex particles but the authors suggested that the value may have been overestimated.[42] In this context, our calculation based on the modeling result seem to be a reasonable estimate of maximum pPEGMA (MW ~ 475) grafting density from flat surfaces.

In methanol/water solutions we were not confident that the solution polymer provided a good indication of the properties of the surface polymer (solution polymer data are presented in the Supporting Information). Therefore, we cannot verify the maximum graft density for these surfaces by the method used above. However, the measured thicknesses (equilibrium brush height Table 3) and the dry layer thickness (Figure 2) taken together provide a measure of the chain stretching. Since we also have these measures for the ethanol solvent system and verified that maximum chain stretching was present, it is possible to plot and compare these two data sets to see if the same degree of stretching was achieved. Figure 8 shows a

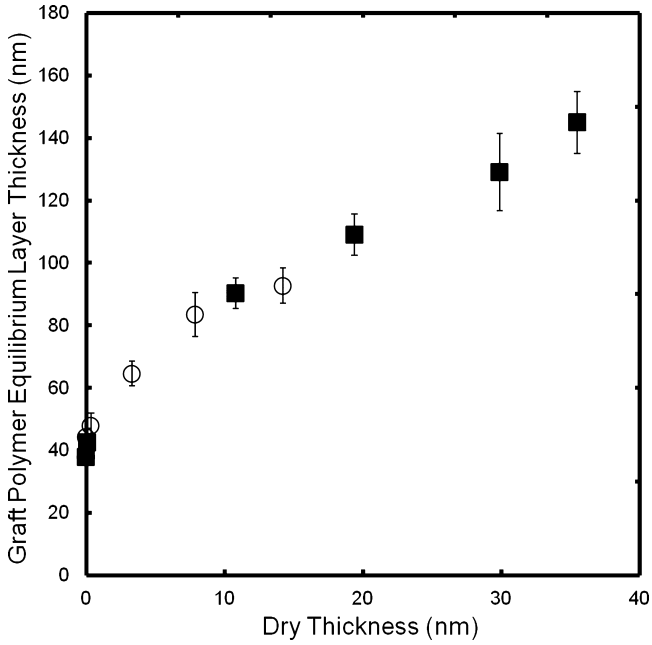

Figure 8. Comparison of polymer chain stretching for pPEGMA brushes grafted from high ATRP abundance initiators in either ethanol/water (■) or methanol/water (○). Layer thicknesses are expressed relative to the plasma polymer layer. Uncertainties represent one standard deviation ($n \approx 20$).

similar trend in either data set. Here we have graphed the hydrated layer thickness relative to the plasma polymer. This emphasizes the fact that the low MW chains formed within the initiator layer contribute to the stretching ratio in a nonlinear way and that only chains long enough to escape this layer to an appreciable degree have a uniform stretching profile. The overlap and linear trend here suggests that polymerization in methanol/water also produced densely grafted pPEGMA brushes of maximum graft density resulting in brush heights near the contour length as was the case for the ethanol solvent system. Therefore, under identical conditions, polymerizations

in methanol−water also appear to have resulted in maximum graft density albeit with a lower molecular weight.

The polarity of alcohol/water mixtures has been shown to influence SI-ATRP of PEGMA. With methanol and water in varying proportions, Feng et al. found that thicker graft layers were obtained as the polarity of the solvent decreased.[48] We have verified this with ethanol/water solutions (not previously compared) and showed that use of the less polar solution resulted in grafted layers greater than twice as thick. The use of water as a cosolvent with alcohol has many advantages for SI-ATRP of PEGMA. First, compared to alcohol alone, water acts as an accelerant, allowing for shorter polymerization times.[48] However, polymerizations carried out in pure water do not allow for controlled polymerization in every case as seen for large, PEG-based monomers such as PEGMA[50] and PEG acrylamide.[42] In our study, 70:30 mixtures of alcohol/water resulted in controlled surface polymerizations but seemed to approach the limit of control at least as far as the solution polymer is concerned. Higher polydispersities resulted as [PEGMA] was increased and this may be due to the fact that at high concentration (approaching 1 M in this study), despite PEGMA having a relatively low mole fraction (6%) the fraction of PEGMA by volume contributes significantly to the total solvent makeup (44%). Therefore the solution polymerization becomes more complicated as it becomes difficult to correlate monomer and catalyst effects in what now must be considered a 3 component solvent system. We also note that Bergnudd et al. show that for the ligand used in this study (HMTETA) polymerization of PEGMA in any number of different solvents may be just on the limit of control.[50] Further refinement of the solution makeup in future studies may result in gaining more control over a wider set of experimental parameters.

Cellular Attachment to Grafted Surfaces. The substrate-independent modification strategy that we have employed allowed the surfaces of polymeric materials of complex geometry (i.e., inside a 96-well microtiter plate) to be grafted with pPEGMA chains in a similar fashion to the flat silicon surfaces shown above. Therefore it was straightforward to translate the high-density graft coating characterized above to materials suitable for cell culture studies. We observed that cells were prevented from attaching to the pPEGMA grafted brush surface preferring to remain rounded in self-associated clusters (Figure 5). This is in contrast to either the initiator or control (TCPS) surface where cell morphology clearly showed attachment and cell spreading. It is the hydrophilic nature of the PEG side chains and the thermodynamic nature of polymer brushes that have already been shown to allow construction of low cell and low protein attaching surfaces that are useful for patterning applications.[6,31,51,53] Our approach, in which we have demonstrated covalent attachment of brushes to many substrates and demonstrated reduced protein adsorption[37] and now show a way of tuning the graft density, seems to be a desirable platform for further research into biomaterial applications.

CONCLUSION

We have demonstrated a method for controlling the graft density for surface-initiated ATRP potentially from any substrate. This was made possible by tuning the initiator quantity in a novel terpolymer ATRP macroinitiator and immobilizing on plasma polymer-treated surfaces. That the abundance of ATRP residues could be reliably tuned and immobilized was verified by NMR characterization of the macroinitiator in solution and then confirmed by XPS when covalently attached to the surface. We prepared both low and high ATRP initiator abundance initiators where the amounts were varied by a factor of 2. SI-ATRP of PEGMA from either surface resulted in low and high graft density surfaces. The layer thickness was able to be varied in a proportional way by varying the concentration of PEGMA in the polymerization solution. Additionally, changing the polymerization solvent from methanol/water to ethanol/water resulted in grafted layers that were greater than twice as thick. The hydrated properties of the grafted surfaces were investigated in solution by using colloid probe microscopy. When present at low density, polymer chains retained some entropic freedom to stretch away from the surface and facilitate bridging interactions with the colloid probe, attracting it to the surface. For the high density case, polymer chains were packed so closely together that chains were forced to stretch to their contour length to avoid entropic penalties associated with crowding. With very little entropic freedom, probe-graft interactions were purely repulsive and provided a useful measure of the equilibrium layer thickness. The hydrated thickness of pPEGMA brushes could be varied regularly in response to the monomer concentration and maximally produced layers over 50 or 100 nm thick depending upon whether methanol/water or ethanol/water was used as the polymerization solvent respectively. We estimated the maximum graft density to be 0.22 chains nm^{-2}. Cells on densely grafted pPEGMA surfaces remained rounded and nonattaching verifying that such grafted surfaces would be useful in biomaterial applications. The method presented also allows for lower density surfaces to be grafted resulting in chain conformations that retain greater entropic freedom and have different physical properties. This is a particularly important to control since experimental[31] and modeling studies[52] have shown that lower graft densities (i.e., lower than the maximum graft density) may confer better stability and antifouling performance for grafted bottle-brush type polymers such as pPEGMA.

ASSOCIATED CONTENT

Supporting Information

Detailed calculation of graft density with discussion of the application of the self-consistent field model to experimental work. Detailed discussion on the mechanism of chain initiation for SI-ATRP from charged surfaces. XPS characterization of grafted layers: S.I. Figure 1 with elemental ratios and S.I. Figure 2 showing C3 component ratio. Solution polymer characterization by GPC/MALLS (S.I. Figure 3). Comparison of sample thickness measurements (S.I. Table 1) by profilometry and XPS overlayer calculations. This material is available free of charge via the Internet at http://pubs.acs.org/

AUTHOR INFORMATION

Corresponding Author

*Tel: +61 8 8302 3152. Fax: +61 8 8302 3683. E-mail: Bryan.Coad@unisa.edu.au.

Notes

The authors declare no competing financial interest.

ACKNOWLEDGMENTS

We acknowledge the Cooperative Research Centre for Polymers for funding (BRC). We are grateful to Dr. Jo

Cosgriff and Dr. Roger Mulder for assistance with NMR and to Mr. Kelly Tsang for assistance with the cell culture studies.

REFERENCES

(1) Pyun, J.; Kowalewski, T.; Matyjaszewski, K., *Polymer Brushes by Atom Transfer Radical Polymerization*; Advincula, R. C., Ed.; Wiley-VCH Verlag GmbH & Co. KGaA: Weinheim, Germany, 2004; pp 51−68.
(2) Edmondson, S.; Osborne, V. L.; Huck, W. T. S. *Chem. Soc. Rev.* **2004**, *33*, 14−22.
(3) Fristrup, C. J.; Jankova, K.; Hvilsted, S. *Soft Matter* **2009**, *5*, 4623−4634.
(4) Xu, F. J.; Neoh, K. G.; Kang, E. T. *Prog. Polym. Sci.* **2009**, *34*, 719−761.
(5) Barbey, R.; Lavanant, L.; Paripovic, D.; Schüwer, N.; Sugnaux, C.; Tugulu, S.; Klok, H.-A. *Chem. Rev.* **2009**, *109*, 5437−5527.
(6) Hucknall, A.; Rangarajan, S.; Chilkoti, A. *Adv. Mater.* **2009**, *21*, 2441−2446.
(7) Raynor, J. E.; Capadona, J. R.; Collard, D. M.; Petrie, T. A.; Garcia, A. J. *Biointerphases* **2009**, *4*, FA3−FA16.
(8) Coad, B. R.; Steels, B. M.; Kizhakkedathu, J. N.; Brooks, D. E.; Haynes, C. A. *Biotechnol. Bioeng.* **2006**, *97*, 574−587.
(9) Mittal, V.; Matsko, N. B.; Butte, A.; Morbidelli, M. *Macromol. React. Eng.* **2008**, *2*, 215−221.
(10) Nagase, K.; Kobayashi, J.; Kikuchi, A. I.; Akiyama, Y.; Kanazawa, H.; Okano, T. *Langmuir* **2008**, *24*, 511−517.
(11) Bruening, M. L.; Dotzauer, D. M.; Jain, P.; Ouyang, L.; Baker, G. L. *Langmuir* **2008**, *24*, 7663−7673.
(12) de Gennes, P. G. *Macromolecules* **1980**, *13*, 1069−1075.
(13) Milner, S. T. *Science* **1991**, *251*, 905−914.
(14) Lai, B. F. L.; Creagh, A. L.; Janzen, J.; Haynes, C. A.; Brooks, D. E.; Kizhakkedathu, J. N. *Biomaterials* **2010**, *31*, 6710−6718.
(15) Schüwer, N.; Geue, T.; Hinestrosa, J. P.; Klok, H.-A. *Macromolecules* **2011**, *44*, 6868−6874.
(16) Ma, H. W.; He, J. A.; Liu, X.; Gan, J. H.; Jin, G.; Zhou, J. H. *ACS Appl. Mater. Interfaces* **2010**, *2*, 3223−3230.
(17) Yamamoto, S.; Ejaz, M.; Tsujii, Y.; Matsumoto, M.; Fukuda, T. *Macromolecules* **2000**, *33*, 5602−5607.
(18) Yamamoto, S.; Ejaz, M.; Tsujii, Y.; Fukuda, T. *Macromolecules* **2000**, *33*, 5608−5612.
(19) Vermette, P.; Meagher, L. *Langmuir* **2002**, *18*, 10137−10145.
(20) Goodman, D.; Kizhakkedathu, J. N.; Brooks, D. E. *Langmuir* **2004**, *20*, 2333−2340.
(21) Goodman, D.; Kizhakkedathu, J. N.; Brooks, D. E. *Langmuir* **2004**, *20*, 6238−6245.
(22) Hamilton-Brown, P.; Gengebach, T.; Griesser, H. J.; Meagher, L. *Langmuir* **2009**, *25*, 9149−9156.
(23) Coad, B. R.; Kizhakkedathu, J. N.; Haynes, C. A.; Brooks, D. E. *Langmuir* **2007**, *23*, 11791−11803.
(24) Zou, Y.; Kizhakkedathu, J. N.; Brooks, D. E. *Macromolecules* **2009**, *42*, 3258−3268.
(25) Riachi, C.; Schüwer, N.; Klok, H.-A. *Macromolecules* **2009**, *42*, 8076−8081.
(26) Zou, Y.; Yeh, P.-Y. J.; Rossi, N. A. A.; Brooks, D. E.; Kizhakkedathu, J. N. *Biomacromolecules* **2010**, *11*, 284−293.
(27) Jiang, X. W.; Chen, H. Y.; Galvan, G.; Yoshida, M.; Lahann, J. *Adv. Funct. Mater.* **2008**, *18*, 27−35.
(28) Wu, T.; Efimenko, K.; Genzer, J. *J. Am. Chem. Soc.* **2002**, *124*, 9394−9395.
(29) Liu, Y.; Klep, V.; Zdyrko, B.; Luzinov, I. *Langmuir* **2004**, *20*, 6710−6718.
(30) Wang, X.; Tu, H.; Braun, P. V.; Bohn, P. W. *Langmuir* **2006**, *22*, 817−823.
(31) Tugulu, S.; Klok, H.-A. *Biomacromolecules* **2008**, *9*, 906−912.
(32) Bao, Z.; Bruening, M. L.; Baker, G. L. *Macromolecules* **2006**, *39*, 5251−5258.
(33) Wang, S.; Zhu, Y. *Langmuir* **2009**, *25*, 13448−13455.
(34) Edmondson, S.; Armes, S. P. *Polym. Int.* **2009**, *58*, 307−316.
(35) Ohno, K.; Kayama, Y.; Ladmiral, V.; Fukuda, T.; Tsujii, Y. *Macromolecules* **2010**, *43*, 5569−5574.
(36) Meagher, L.; Thissen, H.; Pasic, P.; Evans, R. A.; Johnson, G. Method for controllably locating polymerization initiators on substrate surface for forming biological coating involves covalently binding macromolecule to surface having several polymerization initiators and several surface binding groups . WO2008019450-A1; US2008045686-A1; EP2052045-A1; AU2007284002-A1; CN101528876-A; JP2010501028-W, WO2008019450-A1 21 Feb 2008 C09D-201/02 200980, 2008.
(37) Coad, B. R.; Lu, Y.; Meagher, L. *Acta Biomater.* **2012**, *8*, 608−618.
(38) Kizhakkedathu, J. N.; Brooks, D. E. *Macromolecules* **2003**, *36*, 591−598.
(39) Griesser, H. J. *Vacuum* **1989**, *39*, 485−488.
(40) Cleveland, J. P.; Manne, S.; Bocek, D.; Hansma, P. K. *Rev. Sci. Instrum.* **1993**, *64*, 403−405.
(41) Tan, S.; Li, J.; Zhang, Z. *Macromolecules* **2011**, *44*, 7911−7916.
(42) Kizhakkedathu, J. N.; Janzen, J.; Le, Y.; Kainthan, R. K.; Brooks, D. E. *Langmuir* **2009**, *25*, 3794−3801.
(43) Zhao, C.; Li, L.; Wang, Q.; Yu, Q.; Zheng, J. *Langmuir* **2011**, *27*, 4906−4913.
(44) Kingshott, P.; Thissen, H.; Griesser, H. J. *Biomaterials* **2002**, *23*, 2043−2056.
(45) Jayachandran, K. N.; Takacs-Cox, A.; Brooks, D. E. *Macromolecules* **2002**, *35*, 4247−4254.
(46) Janzen, J.; Le, Y.; Kizhakkedathu, J. N.; Brooks, D. E. *J. Biomater. Sci.-Polym. Ed.* **2004**, *15*, 1121−1135.
(47) Kizhakkedathu, J. N.; Norris-Jones, R.; Brooks, D. E. *Macromolecules* **2004**, *37*, 734−743.
(48) Feng, W.; Chen, R. X.; Brash, J. L.; Zhu, S. P. *Macromol. Rapid Commun.* **2005**, *26*, 1383−1388.
(49) Jiang, D.; Huang, X.; Qiu, F.; Luo, C.; Huang, L. L. *Macromolecules* **2010**, *43*, 71−76.
(50) Bergenudd, H.; Coullerez, G.; Jonsson, M.; Malmström, E. *Macromolecules* **2009**, *42*, 3302−3308.
(51) Gautrot, J. E.; Trappmann, B.; Oceguera-Yanez, F.; Connelly, J.; He, X.; Watt, F. M.; Huck, W. T. S. *Biomaterials* **2010**, *31*, 5030−5041.
(52) de Vos, W. M.; Leermakers, F. A. M.; Lindhoud, S.; Prescott, S. W. *Macromolecules* **2011**, *44*, 2334−2342.
(53) Hucknall, A.; Simnick, A. J.; Hill, R. T.; Chilkoti, A.; Garcia, A.; Johannes, M. S.; Clark, R. L.; Zauscher, S.; Ratner, B. D. *Biointerphases* **2009**, *4*, FA50−FA57.